# A Monopole-Probe-Based Quasi-Optical Amplifier Array

Nicholas J. Kolias, *Member, IEEE,* and Richard C. Compton, *Member, IEEE*

***Abstract*— A quasi-optical amplifier array designed for $Ku$-band operation is presented. Orthogonal monopole-probe antennas are used to couple the power into, and out from, an array of microstrip-based amplifiers. The array has a gain of 5.4 dB at 16.4 GHz using packaged high electron mobility transistors (HEMT's). This gain is 3.5 dB below the maximum stable gain for this device at this frequency.**

***Index Terms*— Active antennas, active arrays, FDTD methods, Gaussian beams, lens-focused measurements, microstrip, millimeter-wave amplifiers, millimeter-wave power dividers/combiners, probe antennas, Quasi-optical amplifiers.**

## I. Introduction

A NUMBER of different quasi-optical amplification schemes have been reported for combing the output of large numbers of solid-state amplifiers. These approaches primarily differ in the coupling method used to feed the ensemble of amplifiers. Among the proposed quasi-optical amplifier arrays are grid arrays [1]–[4], slot-based arrays [5]–[7], patch-based arrays [8]–[12], monopole-probe-based arrays [13]–[16], and slab combiners [17], [18].

Grid approaches feature a compact cell size. The proposed amplifier arrays based on slots and patches [5]–[12] need to be significantly larger than the grid arrays to produce the same amount of output power. However, for slot and patch designs, the amplification takes place in a standard transmission-line environment, thereby allowing the use of established coplanar waveguide (CPW) or microstrip multistage amplifier designs.

The monopole-probe-based approach seeks to combine the positive attributes of grid designs and slot/patch designs. Like the grid approach, the probe-based design has two output devices per cell and a high density of devices. Furthermore, the probe approach is amenable to CPW or microstrip-amplifier integration.

## II. Design

The monopole-probe-based amplifier array cell is pictured in Fig. 1. The array design starts with the testing of a single unit cell in a 4-GHz square-waveguide test set [13]. In this step, a number of passive unit cells (unit cells with the transistors replaced with straight through microstrip transmission lines) were tested, and then amplifiers were inserted into the most promising passive cells. The cell with the lowest insertion loss was then scaled to $Ka$-band and duplicated to form the passive array described in [14]. This passive array is similar to the array of Fig. 1, but with the amplifiers replaced by transmission-line feed-throughs. The performance of a passive array gives an indication of how well the incident beam is coupled into, and out from, the input and output antennas. A well-designed array will serve to rotate the polarization of the incident signal with minimal insertion loss. As described in [14], the $Ka$-band passive array rotates the polarization of an incident beam with only 1 dB of insertion loss at 34 GHz and a fractional 3-dB bandwidth of 18%. This array was accurately modeled using a three-dimensional finite-difference time-domain (3-D FDTD) method, as reported in [19].

As shown in Fig. 1, the monopole-probe-based array has an inductive mesh (a square metal grid) on one side of a substrate, which serves as the ground plane for the microstrip lines patterned on the opposite side. Meshes of this type have the frequency characteristic of a low $Q$ bandpass filter [20]–[23], with the transmission band occurring at frequencies just below the Rayleigh frequency of $f_R = c/ng$, where $c$ is the phase velocity of the incident beam, $n$ is the index of refraction of the substrate, and $g$ is the mesh period. A normally incident beam at a frequency within the mesh's bandpass region will excite fields in the mesh apertures, which are predominantly (approaching 100%) the $\mathrm{TE}_{10}$ square-waveguide mode. Thus, by choosing the grid period appropriately, the performance of the cells in the planar design of Fig. 1 will be similar to the square-waveguide performance of [13].

As vertically polarized incident waves strike the mesh, the electric fields which are excited in the mesh apertures are coupled into 50-$\Omega$ microstrip transmission lines through the vertically oriented monopole-probe antennas. The signal is then amplified, rotated in polarization, and finally re-transmitted in the orthogonal polarization. The array is designed to be placed between two orthogonal polarizers [Fig. 1(a)]. The polarizers help to maximize the coupling into, and out from, the antennas, and, in addition, ensure that the input and output beams are cross-polarized, which helps to minimize unwanted feedback. Incident power that is not coupled into the vertical $E$-field probe antennas will be reflected back into the input by the output polarizer. The degree of coupling into the probe antennas is dependent on the spacing $l_1$ and $l_2$ of the meshes away from the array, and the dimensions of the probe antenna [13], [24].

Manuscript received September 20, 1996; revised April 25, 1997. This work was supported by the Army Research Office under Contract DAAH04-94-G-0087.

N. J. Kolias was with the School of Electrical Engineering, Cornell University, Ithaca, NY 14853 USA. He is now with Raytheon Electronics, Advanced Device Center, Andover, MA 01810 USA.

R. C. Compton is with the School of Electrical Engineering, Cornell University, Ithaca, NY 14853 USA.

Publisher Item Identifier S 0018-9480(97)05375-1.

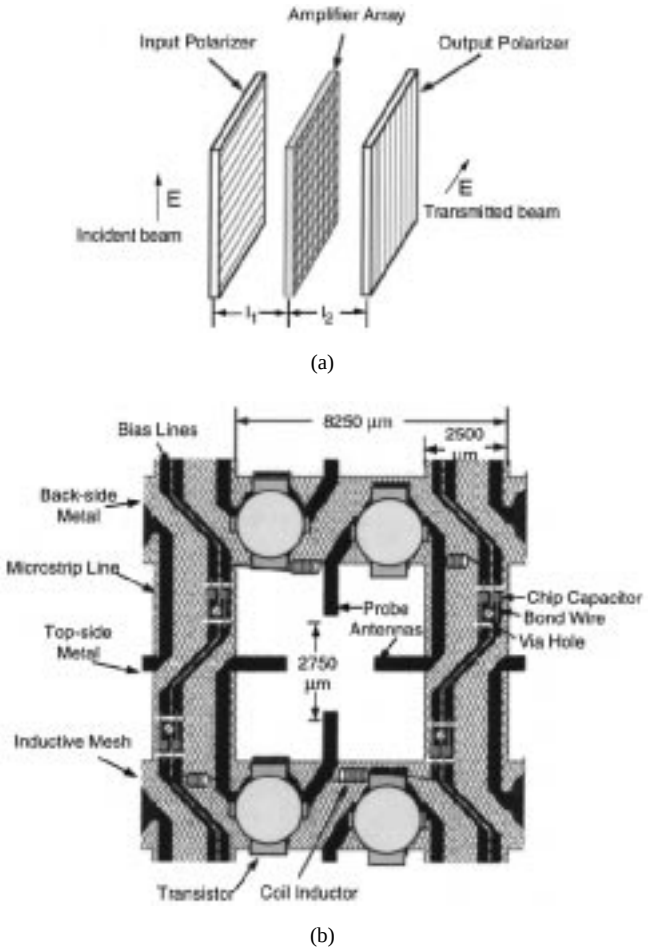


Fig. 1. (a) Probe amplifier array shown, placed between two strip-grating polarizers and (b) optimized monopole-probe-based unit cell showing the positions of the transistors and the biasing networks.

Probe antennas were used because their smaller footprint permits two sets of input and output antennas per cell. This allows for two microstrip amplifier circuits per cell, which effectively doubles the output-power per-unit-array area. Probe antennas also have an advantage over slot/patch designs in terms of loss and efficiency. As demonstrated by waveguide-to-microstrip transitions and waveguide-to-CPW transitions [25]–[27], probe antennas (with an offset backshort) have low loss over a broad millimeter-wave bandwidth when coupling to an incoming beam at normal incidence.

Whereas the $Ka$-band design in [14] is well suited for monolithic fabrication, it is too small to build in hybrid form. For this reason, the $Ka$-band passive array was scaled to $Ku$-band (where fabrication is easier), and packaged Fujitsu high electron mobility transistors (HEMT's) were inserted into the microstrip paths to produce a $Ku$-band active array. Using the FDTD modeling approach of [19], a passive array similar to [14], but scaled for $X$-band operation, was first designed and fabricated with its measured performance shown in Fig. 2. This passive $X$-band array, which was modified to form the active $Ku$-band array, exhibits good agreement with theory and has a peak insertion loss of less than 1 dB and a fractional 3-dB bandwidth of 27.5%. As expected, the reflected power drops down in the frequency region of

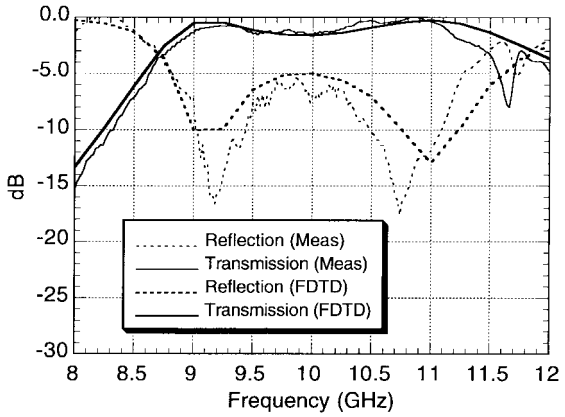


Fig. 2. $X$-band performance of scaled passive array compared with FDTD theory for input and output polarizer spacings of 2 and 4 mm, respectively.

good transmission. The array was tested using the two-port focused-Gaussian-beam method described in [14], [15]. The array was built on 20-mil-thick Rogers TMM-10 substrate with dielectric constant $\epsilon_r = 9.8$, and 1/2-oz (17-$\mu$m) copper metallization. The high dielectric-constant substrate material was chosen to keep the design compatible with eventual monolithic fabrication. This passive array's inductive mesh has a grid period, $g$, of 7750 $\mu$m and a grid linewidth, $2a$, of 2000 $\mu$m. The monopole-probe antennas are 2160-$\mu$m-long and 480-$\mu$m-wide.

This passive $X$-band array was then modified to accommodate the Fujitsu FHX35-LG HEMT's, as shown in Fig. 1. In this modified design, the grid period and linewidth was 8.25 and 2.5 mm, respectively. To reduce feedback between the input and output antennas, the antenna spacing was increased by reducing the antenna length to 1.5 mm. To minimize feedback through the bias lines, the lines are curved and each bias connection is made through a bias-tee network. Each transistor's gate and drain leads are connected to the bias line through an RF-choke inductor. The dc side of the choke inductor is connected to a 43-pF chip capacitor, which acts as an RF-ground. 18-nH choke inductors were used for the gate bias, while for the drain bias, 93-nH inductors were used. These values were arrived at semi-empirically to avoid bias oscillations. The inductors were 18-mil-diameter copper coils. The via holes for the transistors source leads were laser drilled using a Florod Laser Machine. The laser was also used to drill the holes for the vias in the bias lines and to trim the monopole-probe antennas to the optimal length.

## III. Performance

Because of the shorter probe antennas, the active array is expected to have peak performance at slightly higher frequencies than the $X$-band passive array. This was verified by testing a passive version of the array of Fig. 1 at both $Ku$- (12–18 GHz) and X-bands (8–12 GHz). By adjusting the polarizer positions, good rotation could be obtained at frequencies from 10–18 GHz. This agrees well with FDTD simulations, which were done for an array of these dimensions.

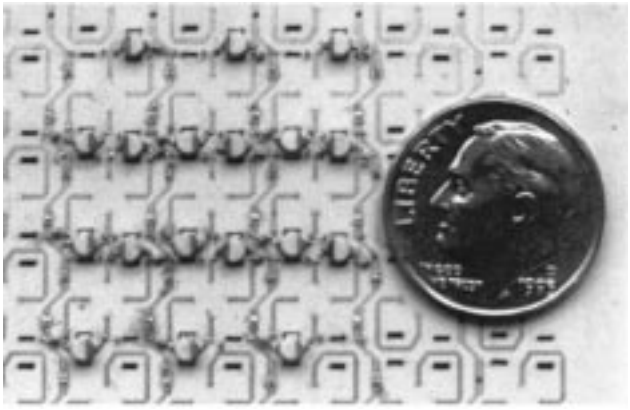

Fig. 3. Photograph of the completed active amplifier array.

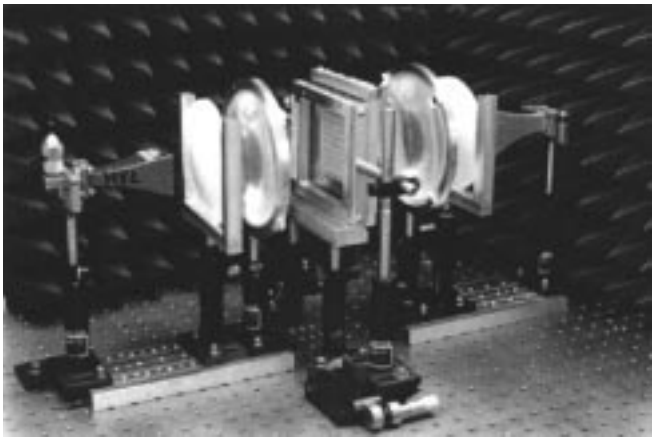

Fig. 4. Photograph of the $Ku$-band focused-Gaussian-beam test setup.

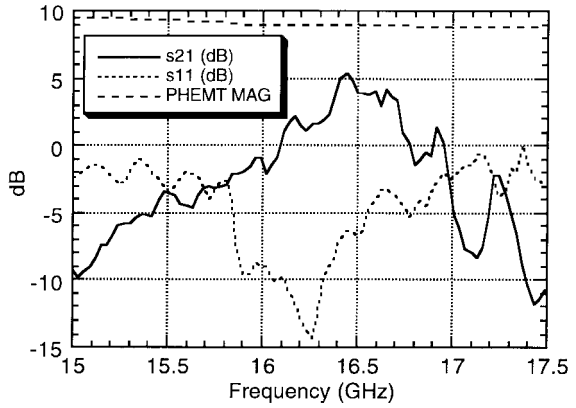


Fig. 5. Measured gain ($s_{21}$) and reflection loss ($s_{11}$) for amplifier array with input and output polarizers spaced from the array surfaces at 9 and 7.5 mm, respectively. For comparison, the HEMT's MAG is also plotted.

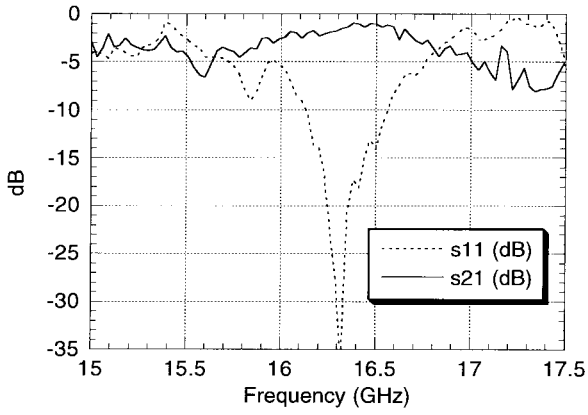


Fig. 6. Measured transmission ($s_{21}$) and reflection ($s_{11}$) for passive array with input and output polarizers spaced from the array surfaces at 9 and 7.5 mm, respectively.

To test the active array, a 3 $\times$ 3 subsection of the array was populated with 18 transistors (2 per cell) and bias wires were attached. The fabricated array is shown in Fig. 3. Ferrite beads were added to the bias wires to avoid low-frequency (MHz) bias oscillations. If these oscillations are not suppressed, the devices, which have considerable low frequency gain, break down. The devices were then gradually biased and the polarizers adjusted to achieve maximum gain. The array measurements were performed with a $Ku$-band focused-Gaussian-beam test setup (Fig. 4) with the beam-waist apertured to the diameter of the 3 $\times$ 3 array subsection. The aperturing of the beam limits any contribution from the nonpopulated passive array cells. A broad-band antenna connected to a spectrum analyzer was placed just above the array to confirm the absence of oscillations.

A maximum gain of 5.4 dB with a 3-dB bandwidth of 2.4% was obtained at 16.4 GHz, as shown in Fig. 5. This measured gain is 3.9 dB less than the maximum available gain (MAG) of a conjugately matched device. The devices in the array have no input/output matching circuitry, although adjusting the polarizer positions tunes the input/output reactance, which the devices see. The data in Fig. 5 was obtained with the input and output polarizers spaced from the array surfaces at 9 and 7.5 mm, respectively. The bias conditions were $V_{\rm gs} = -0.1$ V, $V_{\rm ds} = 0.5$ V, and total $I_{\rm ds} = 165$ mA. This total drain current corresponds to an average drain current of 9.2 mA per device. No oscillations were observed. As a further check for oscillations, this gain was measured at different RF-power levels, thereby, verifying that the output power varied linearly with input power.

However, when the drain voltage is increased over 0.5 V, oscillations begin to appear at 8.9 and 14.1 GHz. These oscillations indicate the presence crosstalk and feedback between adjacent amplifier elements. It should be noted that when a single transistor in an array cell is biased alone, no oscillations are observed—even at high bias levels. To operate at the higher bias levels where the gain is higher and oscillations occur, the adjacent elements must be spaced further apart, or alternatively, resistors which effectively reduce the transistors' gain could be placed in the transistor gate and/or drain paths, as done in the grid arrays [1]–[4]. However, because the addition of resistors reduces device gain, this approach may not yield additional total gain.

Fig. 6 shows the passive-array performance of this design with input and output polarizers at the same positions as in Fig. 5. The frequencies of maximum gain between 16.1 and 16.7 GHz for the active array correspond to dips in the reflection coefficient $s_{11}$, for both the active and passive arrays, and correspondingly good transmission for the passive array.

## IV. Conclusion

A $Ku$-band active-amplifier array based on the passive microstrip $Ka$-band array of [14] has been described. A passive array was first designed and tested. This scaled passive array exhibited excellent performance with an insertion loss of less than 1 dB and a 3-dB bandwidth of 27.5%. These results agree well with FDTD simulations. Transistors were then added to the passive array to obtain 5.4 dB of gain at 16.4 GHz.

## Acknowledgment

The authors would like to thank Rogers Corporation for donating the TMM-10 substrates and Microwave Components, Inc., for donating the inductors used in this work.

## References

[1] M. Kim, J. J. Rosenberg, R. P. Smith, R. M. Weikle, II, J. B. Hacker, M. P. Delisio, and D. B. Rutledge, "A grid amplifier," *IEEE Microwave Guided Wave Lett.*, vol. 1, pp. 322–324, Nov. 1991.

[2] M. Kim, E. A. Sovero, J. B. Hacker, M. P. Delisio, J. Chiao, S. Li, D. R. Gagnon, J. J. Rosenberg, and D. B. Rutledge, "A 100-element HBT grid amplifier," *IEEE Trans. Microwave Theory Tech.*, vol. 41, pp. 1762–1771, Oct. 1993.

[3] C. Liu, E. A. Sovero, M. P. Delisio, A. Moussessian, J. J. Rosenberg, and D. B. Rutledge, "Gain and stability models for HBT grid amplifiers," in *IEEE AP-S Int. Symp. Dig.*, June 1995, pp. 1292–1295.

[4] M. P. Delisio, S. W. Duncan, D. Tu, C. Liu, A. Moussessian, J. J. Rosenberg, and D. B. Rutledge, "Modeling and performance of a 100-element PHEMT grid amplifier," *IEEE Trans. Microwave Theory Tech.*, vol. 44, pp. 2136–2144, Dec. 1996.

[5] H. S. Tsai, M. J. W. Rodwell, and R. A. York, "Planar amplifier array with improved bandwidth using folded-slots," *IEEE Microwave Guided Wave Lett.*, vol. 4, pp. 112–114, Apr. 1994.

[6] H. S. Tsai and R. A. York, "Quasi-optical amplifier array using direct integration of MMIC's and 50-$\Omega$ multislot antennas," in *IEEE MTT-S Int. Microwave Symp. Dig.*, May 1995, pp. 593–596.

[7] J. Hubert, J. Schoenberg, and Z. B. Popović, "High-power hybrid quasi-optical $Ka$-band amplifier design," in *IEEE MTT-S Int. Microwave Symp. Dig.*, May 1995, pp. 585–588.

[8] T. Mader, J. Schoenberg, L. Harmon, and Z. B. Popović, "Planar MESFET transmission wave amplifier," *Inst. Elect. Eng. Electron. Lett.*, vol. 29, pp. 1699–1701, Sept. 1993.

[9] J. Schoenberg, S. C. Bundy, and Z. B. Popović, "Two-level power combining using a lens amplifier," *IEEE Trans. Microwave Theory Tech.*, vol. 42, pp. 2480–2485, Dec. 1994.

[10] N. Sheth, T. Ivanov, A. Balasubramaniyan, and A. Mortazawi, "A nine HEMT spatial amplifier," in *IEEE MTT-S Int. Microwave Symp. Dig.*, May 1994, pp. 1239–1242.

[11] T. Ivanov and A. Mortazawi, "Two stage double layer microstrip spatial amplifiers," in *IEEE MTT-S Int. Microwave Symp. Dig.*, May 1995, pp. 589–592.

[12] ———, "A two-stage spatial amplifier with hard horn feeds," *IEEE Microwave Guided Wave Lett.*, vol. 6, pp. 88–90, Feb. 1996.

[13] N. J. Kolias and R. C. Compton, "A microstrip-based unit cell for quasi-optical amplifier arrays," *IEEE Microwave Guided Wave Lett.*, vol. 3, pp. 330–332, Sept. 1993.

[14] ———, "A microstrip-based quasi-optical polarization rotator array," in *IEEE MTT-S Int. Microwave Symp. Dig.*, May 1995, pp. 773–776.

[15] ———, "A 35-GHz CPW-based antenna array for quasi-optical amplifiers," in *20th Int. Conf. Infrared and Millimeter Waves*, Dec. 1995, pp. 151–152.

[16] N. J. Kolias, *Monopole Probe Based Millimeter-Wave Quasi-Optical Amplifier Arrays*, Ph.D. dissertation, Dept. of Elect. Eng., Cornell University, Ithaca, NY, 1996.

[17] H.-S. Hwang, T. W. Nuteson, M. B. Steer, J. W. Mink, J. Harvey, and A. Paolella, "A quasi-optical dielectric slab power combiner," *IEEE Microwave Guided Wave Lett.*, vol. 6, pp. 73–75, Feb. 1996.

[18] A. R. Perkons and T. Itoh, "A 10-element active lens amplifier," in *IEEE MTT-S Int. Microwave Symp. Dig.*, June 1996, pp. 1119–1122.

[19] A. Alexanian, N. J. Kolias, R. C. Compton, and R. A. York, "3-D-FDTD analysis of quasi-optical arrays using floquet boundary conditions and Berenger's PML," *IEEE Microwave Guided Wave Lett.*, vol. 6, pp. 138–140, Mar. 1996.

[20] R. C. McPhedran, G. H. Derrick, and L. C. Botten, *Electromagnetic Theory of Gratings.* Berlin, Germany: Springer, 1980, ch. 7, pp. 227–276.

[21] R. C. Compton and D. B. Rutledge, "Approximation techniques for planar periodic structures," *IEEE Trans. Microwave Theory Tech.*, vol. MTT-33, pp. 1083–1088, Oct. 1985.

[22] C. Chen, "Transmission through a conducting screen perforated periodically with apertures," *IEEE Trans. Microwave Theory Tech.*, vol. MTT-18, pp. 627–632, Sept. 1970.

[23] M. S. Durschlag and T. A. DeTemple, "Far-IR optical properties of freestanding and dielectrically backed metal meshes," *Appl. Opt.*, vol. 20, pp. 1245–1253, Apr. 1981.

[24] G. L. Ragan, *Microwave Transmission Circuits*, (MIT Radiation Laboratory Series, vol. 9). New York: McGraw-Hill, 1948.

[25] Y.-C. Shih, T.-N. Ton, and L. Q. Bui, "Waveguide-to-microstrip transitions for millimeter-wave applications," in *IEEE MTT-S Int. Microwave Symp. Dig.*, May 1988, pp. 473–475.

[26] J. Machac and W. Menzel, "On the design of waveguide-to-microstrip and waveguide-to-coplanar line transitions," in *IEEE MTT-S Int. Microwave Symp. Dig.*, May 1988, pp. 473–475.

[27] F. Chen and W. B. Dou, "Full-wave analysis of waveguide-to-microstrip transitions for millimeter wave applications," *Int. J. Infrared Millim. Waves*, vol. 16, no. 3, pp. 641–652, 1995.

**Nicholas J. Kolias** (S'90–M'96) was born in Endicott, NY, on September 4, 1968. He received the B.S. (with distinction), M.S. and Ph.D. degrees, all in electrical engineering, from Cornell University, Ithaca, NY, in 1990, 1993, and 1996, respectively.

Upon graduation from Cornell, he took a position with the Raytheon Company as a Senior Scientist in their research laboratories. His current research interests are in the areas of millimeter-wave circuit and antenna design.

Dr. Kolias is a member of Tau Beta Pi and Eta Kappa Nu.

**Richard C. Compton** (S'84–M'87) received the Ph.D. degree from the California Institute of Technology, Pasadena, in 1987, where he worked as a Fulbright Scholar on millimeter and microwave arrays.

He is currently an Associate Professor of electrical engineering at Cornell University, Ithaca, NY, where his group builds novel millimeter-wave integrated circuits. He is also a Manager in Hewlett-Packard's Wireless Systems Group, Cupertino, CA. He co-developed the interactive microwave CAD package, Puff, which has over 15,000 copies distributed worldwide. Other products that he has helped to develop include indoor wireless systems for home-lighting control, as well as millimeter-wave radios for point-to-multipoint applications.

Dr. Compton is a National Science Foundation Presidential Young Investigator. In 1994, he served on the Federal Communication Commission's 28-GHz Negotiated Rulemaking Committee.